ELSEVIER

Materials Science and Engineering C 7 (2000) 119–128

MATERIALS SCIENCE & ENGINEERING C

www.elsevier.com/locate/msec

Nano-mechanical properties profiles across dentin–enamel junction of human incisor teeth

Hanson Fong [a], Mehmet Sarikaya [a,*], Shane N. White [b], Malcolm L. Snead [c]

[a] *Materials Science and Engineering Department, University of Washington, Roberts hall, FB-10, Seattle, WA 98195 USA*
[b] *School of Dentistry, UCLA, Los Angeles, CA 90095 USA*
[c] *Center for Craniofacial Molecular Biology, University of Southern California, Los Angeles, CA 90033 USA*

Received 25 January 1999; received in revised form 20 September 1999; accepted 12 October 1999

Abstract

Understanding how load is transferred from enamel to dentin and how the two tissues function as a single mechanical unit during mastication requires studies of micromechanics in relation to microstructure of the dentin–enamel junction (DEJ) zone. In this investigation, nano-hardness and elastic modulus of human incisor teeth were studied across the DEJ. It was found that, over a length scale of about 20 μm, there were decreasing trends in both hardness and elastic modulus across the DEJ zone profiling from enamel to dentin. Images obtained using atomic force microscopy from polished surfaces of cross-sectioned dental samples showed an interpenetrated microstructure of enamel and dentin at the DEJ zone. This result suggests that the nano-mechanical property profiles across the DEJ were due to a continuous variation in the ratios of relative amount of enamel and dentin. These characteristics of the DEJ zone could be significant for describing the structural and mechanical coupling of the two tissues. By increasing the contact area across the interface between the two hard tissues the stresses are dissipated reducing interfacial stress concentrations at the DEJ, thereby promoting effective load transfer from the hard (brittle) enamel to soft (tough) dentin.

Keywords: Enamel; Dentin; DEJ; Nano-mechanical; Hardness

1. Introduction

Dentin and enamel are the two dental tissues that are functionally organized to provide an integrated mechanical system in the human tooth [2]. [1] Over the years, our knowledge has separately increased for the individual tissues and mechanical properties of dentin and enamel. However, data have been insufficient on how these structurally and morphologically different tissues are coupled to provide the tooth with its functional properties as a single mechanical unit [3]. The experimental work presented here was undertaken to obtain detailed mechanical property data across the dentin–enamel junction (DEJ) in order to provide a better insight into the nature of micromechanical integration of these hard tissues.

In the human tooth, enamel is the outer structure that envelops the crown. It is almost fully mineralized with highly organized hydroxyapatite (HAP) crystallites, making it mechanically hard and highly resistant to wear. Dentin is the supporting structure that lies underneath enamel and it is primarily composed of HAP mineralized collagenous matrix surrounding tubular extensions of the dentinoblast cells. This less mineralized tissue provides the tooth with the toughness required to resist catastrophic fracture when subjected to masticatory stresses [1–3].

For more than 60 years, studies have been made to better understand the mechanical properties of these composite materials [1–13]. These studies relied on flexural or tensile tests (bulk scale) [2,6–9] and micro-indentation or nano-indentation (micro- to nanometer scales) [1,2,10–13]. While bulk-scale tests provided results that reflected the overall mechanical response of the tooth when subjected to external load, micro- to nanometer-scale tests revealed information on the hierarchical micromechanics which provide the underlying control mechanisms that lead to the

* Corresponding author. Tel.: +1-2065430724; fax: +1-2065436381; e-mail: sarikaya@u.washington.edu

[1] For instance, see Ref. [1].

0928-4931/00/$ - see front matter
PII: S0928-4931(99)00133-2

overall mechanical response of the tooth. In particular, prior limitations in analytical strategies have resulted in incomplete understanding of the enamel–dentin composite structure. For example, flexural and tensile tests were typically made on notched samples [6–9] using a blunt crack. Nevertheless, the results generally demonstrated that dentin is tougher than enamel and that dentin fractures more anisotropically than enamel [3,6–9]. For example, tensile test on Chevron-notched bovine teeth revealed that dentin was tougher than enamel and that the former underwent plastic deformation while the latter did not [9]. It was also observed that there was a significant increase in resistance to crack propagation at the DEJ zone [9].

Indentation test results revealed mechanical properties that are more directly related to the local structure of the tooth. Early hardness measurements showed that enamel was approximately five times as hard as dentin (3.43 vs. 0.68 GPa Knoop) [4,5]. Due to the large indentation size in comparison to microstructure, however, in these studies only a general trend in hardness was established from surface of the tooth to dentin region. With the advent of nano-indentation instruments with continuous depth sensing capability, detailed studies on hardness, as well as elastic modulus, in relation to tooth microstructure became possible [10–13]. For example, by using a diamond tip attached to a stainless steel cantilever in an atomic force microscope (AFM), the hardness difference between peritubular and intertubular dentin was measured with the load of up to 268 μN [11]. It was reported that hardness of peritubular dentin was approximately four times (2.3 GPa) that of intertubular dentin (0.5 GPa) demonstrating that the former is more mineralized than the latter [11]. The effect of microstructure on crack propagation in enamel due to microindentation was also examined, and it was found that cracks propagated further in the direction perpendicular to the occlusal surface than parallel in the axial section of premolar teeth [12]. Furthermore, it was also found that crack propagation was always arrested at the DEJ [12], which was in agreement with the reported tensile test results [9]. Strain distribution within human tooth was also studied and the results were correlated with its detailed composite structure [13].

In previous studies, it was found that there is an overlap between dentin and enamel structure. For example, a scanning electron microscopy (SEM) study reported that collagen fibrils actually penetrate across the DEJ from dentin to enamel [14]. In our preliminary investigation of the microstructure by transmission electron microscopy (TEM) [15], we found that dentin and enamel tissues posses an interpenetrating interface, rather than a simple planar one. Although data giving detailed three-dimensional structures are still lacking, previous results suggested structural coupling between dentin and enamel through interpenetration of the two phases that would enable strong bonding across this interface. Therefore, over a finite length scale across the DEJ it is expected that there would be a variation in mechanical properties, corresponding to the structural change, across this transition zone. In addition to the limited data available in the literature on the structure, there is a also a lack of data on the corresponding local mechanical properties at the transition zone. The objective of the current research was to investigate this important structural region in human teeth and to obtain detailed (local) mechanical property profiles through its thickness from enamel surface to interior of dentin including the interface region across the DEJ. It was expected that the knowledge of spatially-varying property profiles would provide a quantitative framework upon which future composite modelling of the overall tooth structure could be developed.

We performed nano-indentation tests using the vertical-loading mode that was provided by a nano-indentation apparatus attached to an AFM. At the same time, we used the imaging capabilities of the AFM to control the indenter position on local regions of the sample with high precision. By doing so, a major difficulty associated with previous nano-indentation studies was overcome. In traditional hardness measurements, the location of the indentation is not precisely known because of the lack of an on-line imaging capability in these systems [16]. On the other hand, although AFM has excellent imaging capabilities, nano-indentation measurements with a horizontal AFM cantilever may suffer from a significant measurement error (20–50%) due to a lack of accurate knowledge of cantilever spring-constant and, therefore, in the actual load transfer to the sample upon indentation [16,17]. Additionally, AFM tests suffer from the limitations in loading capabilities, since AFMs offer loads only in the maximum range of 100s of nN while μN-level loads are required in the tests. As indicated above, in our nano-mechanical testing system (see Section 2), the positioning of the tip is achieved by the imaging capabilities of the AFM which allows controlled location of the indentor at a desired position on the sample using the indenter tip as the imaging probe. In fact, imaging can be performed before and after a nano-indentation test; this provides a unique means to investigate deformation behavior of the sample upon indentation. The nano-indentation apparatus allows the application of loads from a few hundred μN up to mN, wide enough range for quantitative analysis of dental hard tissues. It also provides high precision measurements because the load is applied to a vertical indentor and is transferred through a metallic shaft onto a diamond indentation tip. This eliminates a possible problem associated with the compliance of the indentor and provides high precision values of hardness and modulus [16,17]. Furthermore, in this approach, through practice, it is possible to select an indentation size such that it is small enough to resolve the difference in mechanical properties in local regions at the micrometer and nanometer scales, and large enough to represent the general properties of the microstructures with high statistical accuracy.

2. Experimental procedures

2.1. Sample preparation

Adult human incisor teeth were used in this research. Six different teeth were selected from six individuals (originally prepared for microhardness testing) [18]. The samples were sectioned in half along the axial direction and preserved in phosphate buffer saline (PBS) with 0.5% thymol solution. To prepare for indentation, one section of the tooth sample was cold-mounted in an epoxy with the internal side facing out (Fig. 1). An axially sectioned structure of an incisor tooth is displayed in a light-optical microscope image in Fig. 1a (note the corresponding coordinates in Fig. 1b). The cross-section clearly reveals pulp (P), dentin (D), and enamel (E) regions, with a darker line of contrast that represents the DEJ region between dentin and enamel. The sample surface was polished sequentially with 6-, 3-, 1- and 0.25-μm diamond paste. Between polishing steps, the sample was ultrasonically cleaned in de-ionized water to remove any polishing debris. The root mean square (rms) roughness variation, as measured by AFM in the contact-mode, was 5.0 nm or less in local test areas of all samples. The polished samples were preserved in PBS solution until immediately before nano-indentation tests. All the nano-indentation tests were performed in air.

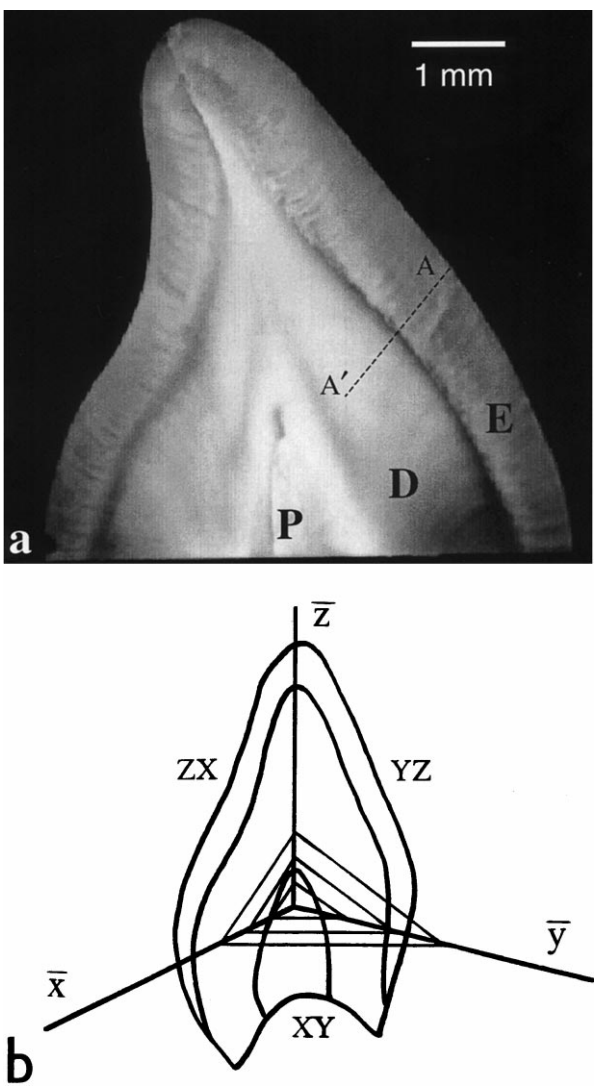

Fig. 1. (a) Image of an axial cross-section of a human incisor sample displaying pulp (P), dentin (D) and enamel (E) regions. Dotted line A–A′ is a representative location of nano-hardness profiles determined in this work (axial section perpendicular to facial and lingual surfaces). (b) A schematic illustration of a section of a human tooth and the corresponding geometry on an orthogonal axes system (section convention used — *YZ*: facial; *ZX*: distal; *XY*: incisal; − *YZ*: lingual; − *ZX*: mesial; − *XY*: basal).

2.2. Indentation and AFM procedures

Indentation was performed with a Hysitron® Picoindentor (a nano-mechanical testing apparatus) attached to a Park® CP scanning probe microscope (SPM). A Berkovich diamond tip, with {111} surfaces forming a triangular pyramid of the diamond single crystal, was used both as an imaging probe and as an indenter. With the nano-indentation apparatus/AFM system, surface topography imaging as well as indentation could be performed sequentially at the same position allowing the analysis of the surfaces before and after indentation tests. For indentation, force (F) vs. displacement (d) of the load–unload cycle was measured. Hardness, H, and reduced elastic modulus, E, were determined from the unloading portion of force–displacement curves with a known indenter tip area function (the tip area is the interface between the tip surface and the surface of sample indented). The tip area function was calibrated with a fused-silica sample according to the procedure described in Ref. [16]. Hardness and reduced elastic modulus determined from the Hysitron® nano-mechanical system is deduced from the following relations:

$$S = P_{\max}/A; \quad E = S(\pi)^{1/2}/2\,A^{1/2},$$

where $P_{\max}$ is the maximum applied load and S is the stiffness of the system. Area of contact, A, is calibrated as a function of contact height, h. For this study, A was calibrated for h values up to 100 nm.

Indentations were performed in air. To prevent extensive drying, exposure to air was minimized (the longest exposure of the teeth to air was about 45 minutes in about 80–100% humid atmosphere). Indentations were carried out on the axially cross-sectioned teeth samples from the surface (enamel) to the interior (dentin) region. At least three profiles were taken for each tooth, all parallel to the direction of natural loading of the teeth. The approximate locations of the indentation profiles in the sectioned teeth on the axial (ZX) plane are shown in Fig. 1a. For each profile, indentations were at least 50 μm apart in most of

the enamel and dentin regions as they showed no significant change in hardness or elastic modulus within this dimensional interval in either of the tissues. However, within a 50 μm of the DEJ, indentations were at least three indent diameters apart (separation ~4 μm) to improve the spatial resolution of the nano-mechanical property profiles. This value of separation between the indents was also large enough to eliminate the possibility of overlap between the successive indentations that would affect the test results. The applied load was varied from 300 to 2500 μN until a contact depth of ~100 nm was maintained both in dentin and enamel to obtain a consistent indentation with a reasonably large sampled area in both tissues. In other words, in both tissues, the total indentation–tip/sample contact surfaces were similar so that the same tip area function calibration could be used. This necessarily caused the loads used in dentin and enamel tests to be different. However, the applied loads chosen were sufficiently high in each of the hard tissues to sample within the smallest composite-structural feature for analysis; rods in enamel and collagen/HAP mixture in dentin. A loading rate of 5 s to maximum load, then an unloading rate of 5 s to zero load were used. These values were selected as they were found to be the maximum rates to eliminate any observable creep.

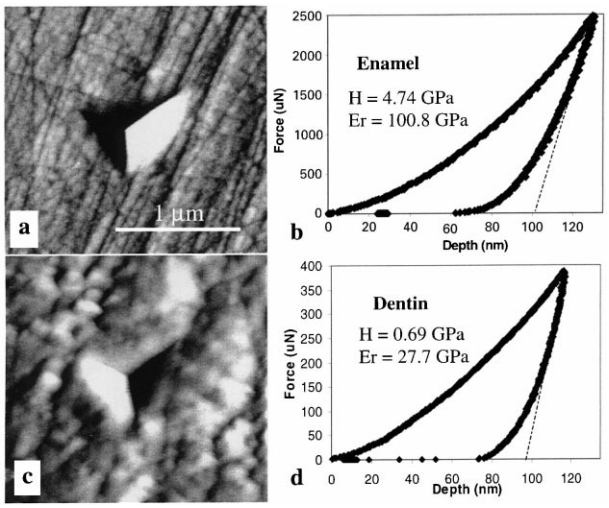

Fig. 3. AFM images of a typical indentations in (a) enamel and (c) in dentin, and the corresponding $F-d$ curves in (b) and (d), respectively.

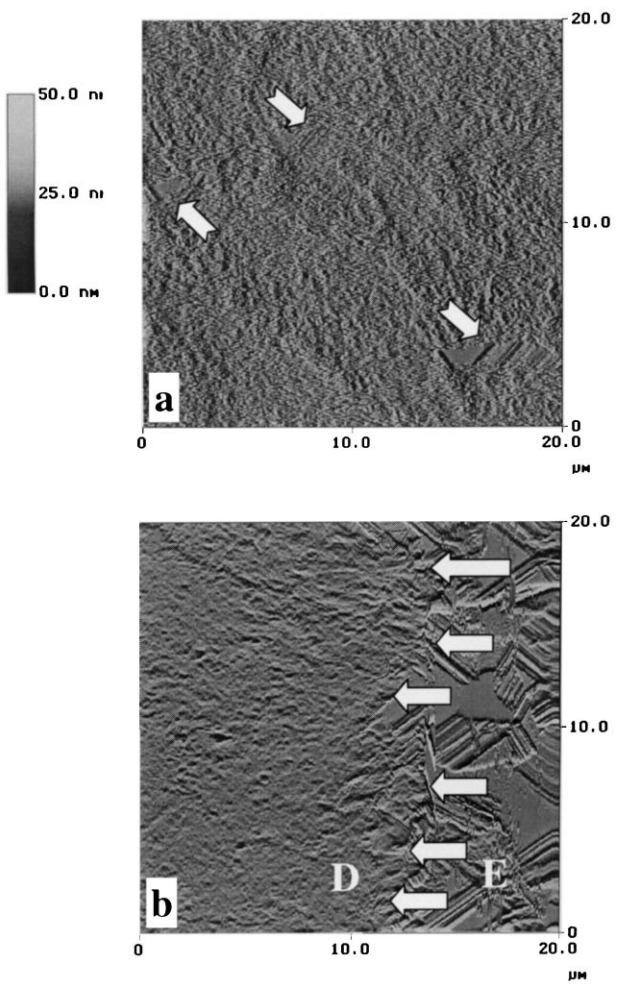

Fig. 2. AFM images of a DEJ (contact mode). (a) Dentin. (b) DEJ region (arrows indicate the approximate position of the interface); E: enamel, and D: dentin.

Surface structures of the teeth were also scanned by the AFM (e.g., see Fig. 2) in the vicinity of the DEJ to reveal structural features in dentin (Fig. 2a) and at the transition zone (Fig. 2b). The polished sample was etched by 2 vol.% HNO_3 in de-ionized water for 20 s. The DEJ zone, as well as dentin and enamel regions, was then scanned in contact-mode by Nanoscope III® SPM from Digital Instrument. Fig. 3 displays characteristic AFM images of indentations (a and c) and the corresponding to force–depth (F–d) curves of dentin and enamel regions (b and d, respectively) recorded under optimum loading conditions (see discussion below). In Fig. 3a and c, the pyramidal shapes of the indents are clearly displayed. The clarity of the diamond indenter's shape in both of the tissues is reflective of the reliability of the experimentally determined mechanical property values since the total stress for hardness determination is derived from the applied load over an area corresponding to a pyramidal impression. Imaging of the indents and their shapes were necessary to ensure the reliability index of the hardness determination (see also Fig. 5b).

3. Results

Measurements were made (along $\bar{x}$ direction, Fig. 1b) in enamel and dentin away from the surface of the teeth

and the DEJ zone to obtain representative nano-mechanical properties in each tissue. This allowed the evaluation of the average values of hardness and elastic moduli of the respective regions and their comparison with those found in the literature. The indentation data were taken from, at least, 30 points in enamel and dentin from each of the six tooth samples used. The average values of hardness measured were 4.79 ± 0.21 and 0.79 ± 0.04 GPa in enamel and dentin, respectively. Corresponding to these measurements, the average elastic moduli of the six teeth samples were 98.3 ± 5.9 and 24.8 ± 1.4 GPa in enamel and dentin, respectively. Nano-mechanical tests were also conducted on *XY* (incisal) section in enamel; the hardness and modulus results provided similar values as tests performed on *ZX* (distal) section (refer to Fig. 1b for the geometry of the sample sectioning). These values for enamel and dentin tissues are comparable to those reported in the literature [9]. It should be noted, however, that there were also observed variations in H values, especially in enamel region and, for example, values as low as 2.3 GPa were encountered. These low values of H were not considered to represent actual hardness of enamel, but rather as artefacts from sample polishing or variations in local structures (e.g., rod interfaces).

Nano-hardness tests were also carried out on one of the prism faces (a or b) of a large single crystal geological apatite mineral for comparison with the values obtained from the composite HAP/organic matrix composites of dentin and enamel. Although enamel is a nano-composite of HAP crystallites (constituting more than 95% of the volume), as shown in Table 1, it is approximately 60% as hard and 80% as rigid as the mineral apatite. However, compared to a single crystal mineral apatite, nano-mechanical property values are significantly lower in dentin in which organic matrix constitutes more than 50 vol.% of the composite structure.

We next determined profiles of the mechanical properties across the DEJ regions in all of the samples. For this, similar scale of loads (300 to 2500 μN) were used as in average bulk *H* and *E* determinations. Hardness and elastic modulus profiles, respectively, in the vicinity of the DEJ are plotted in Fig. 4a through f, Fig. 5a and c. Here, the horizontal axis represents an approximate position of indentations taken with respect to the center of the DEJ zone; this was determined based on the imaging features of the sample. The positions of indentations could be controlled precisely using the AFM's imaging capability using the indenter as the imaging probe. An image obtained this way is shown in Fig. 5b corresponding to the region where the hardness profiles (in Fig. 5a and c) were recorded. In general, in all profiles, one can see changes of hardness and elastic modulus values across the DEJ region. Although the exact center position of the DEJ could not be determined from the profiles, pure dentin or pure enamel tissue could be deduced from the AFM images because these individual tissues display either a fairly smooth surface (enamel) or somewhat rougher surface (dentin) (see Fig. 5b as an example). As seen in all profiles, there is a specific trend of a decrease in both H and E across the DEJ from enamel to dentin. This decrease is continuous through the DEJ zone as a step function. From the average width of the step, the approximate width of the DEJ zone width was measured to be about 20 μm, but the width usually varies between 15 and 25 μm.

It should be noted that the profile of either hardness or elastic modulus measured in the vicinity of DEJ was not always a smoothly varying step-function in all regions and in all samples tested. In some cases the step in a given profile would be sharp over the DEJ; in some other cases, the profile would fluctuate. Furthermore, within a given tissue (i.e., dentin or enamel), the relative amounts in *H* or *E* values could vary from one test point to the next. Regardless of these discrepancies, the overall shape of the profile appears to be reproducible, revealing a finite width of the DEJ region in all of the teeth samples tested. The variations in the nano-mechanical property measurements could reflect structural variations in the respective tissues, such as local content of the HAP or organic matrix material, texture of the HAP crystallites, or the relative orientation of the enamel rods (end-on vs. edge-on).

In order to better correlate the microstructure to the measured nano-mechanical properties at the DEJ zone, AFM scans were performed on the etched samples to reveal details of the underlying structure in the DEJ regions more clearly. As an example, the AFM image of the DEJ zone shown in Fig. 2 reveals that there is a significant amount of overlap between dentin and enamel regions. The sampled areas shown in Fig. 2a and b were next to each other, and the arrows in (a), i.e., dentin, reveal fairly flat local features representative of highly-textured HAP crystallites in enamel. This would indicate that the two tissues somewhat interpenetrate into each other. The extend of overlap of the two tissues is not yet fully quantified and requires a more detailed AFM investigation of etched-samples that would be sectioned in many geometrical projections. It could also be possible to study the DEJ zone in more detail using TEM at relatively low magnifications, which would reveal pseudo-three-dimensional images of

Table 1
Average hardness and elastic modulus values of enamel, dentin, and geological apatite single crystal

	Hardness (GPa)	Elastic modulus (GPa)
Adult incisor tooth		
Enamel incisoral (*XY*)	4.78 ± 0.36	98.3 ± 5.9
Enamel axial (*YZ*)	4.53 ± 0.26	95.6 ± 4.9
Dentin (*YZ*)	0.79 ± 0.04	24.8 ± 1.4
Geological apatite (prism plane)	7.5 ± 1.10	124.6 ± 7.3

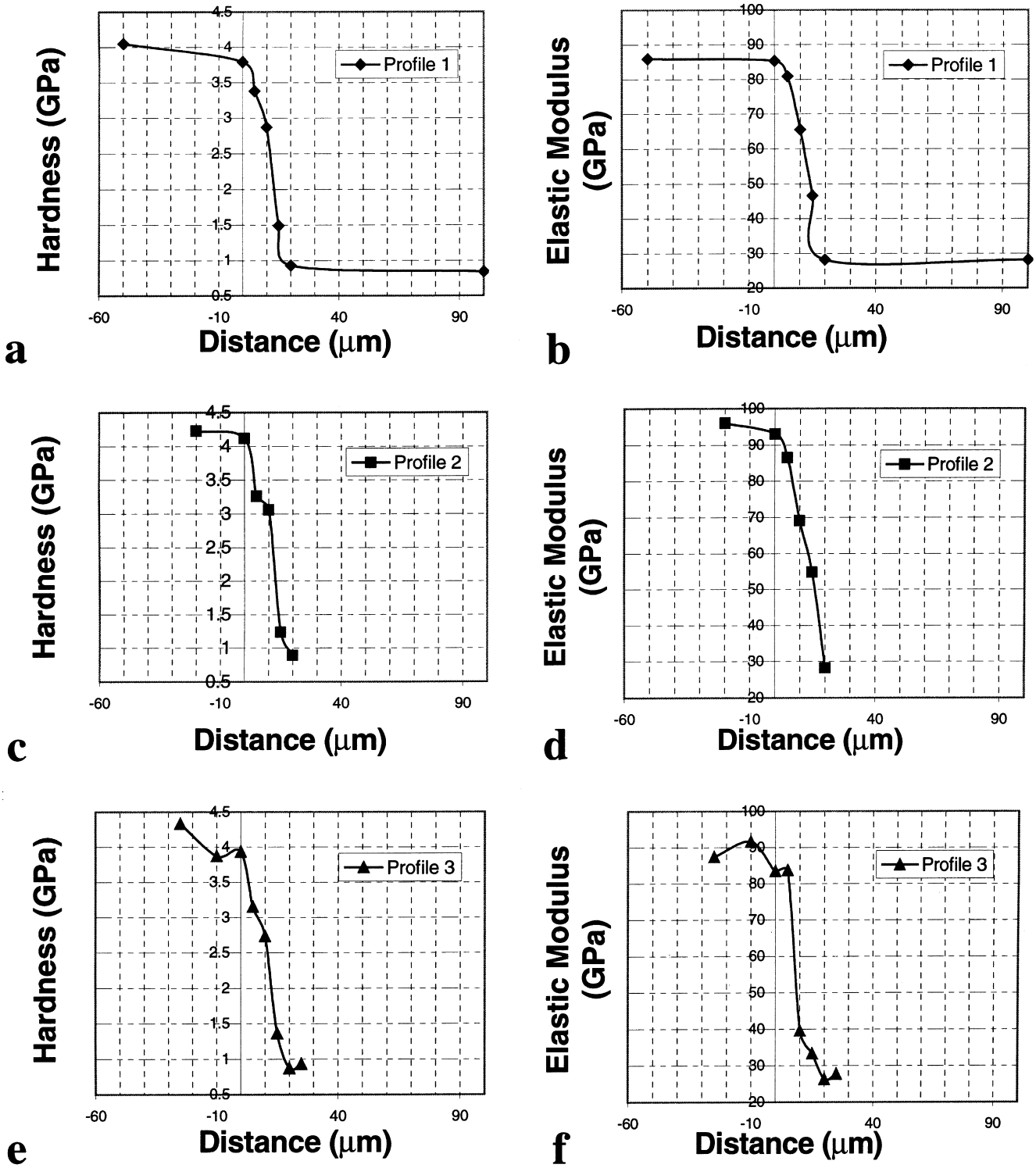

Fig. 4. Nano-mechanical property profiles at several positions across DEJ in human incisor teeth: (a) nano-hardness, and (b) elastic modulus.

many ultramicrotomed sections. Nonetheless, the trends seen in the *H* and *E* profiles obtained to date via the nano-mechanical tests from the sectioned teeth samples suggest a finite width of the DEJ region that can clearly be correlated to the overlapped structures of dentin and enamel.

4. Discussions

There are three factors to consider in determining the reliability of the indentation results: (i) surface roughness of the sample, (ii) overlapping of adjacent indentations of successive measurements and their proximity to mi-

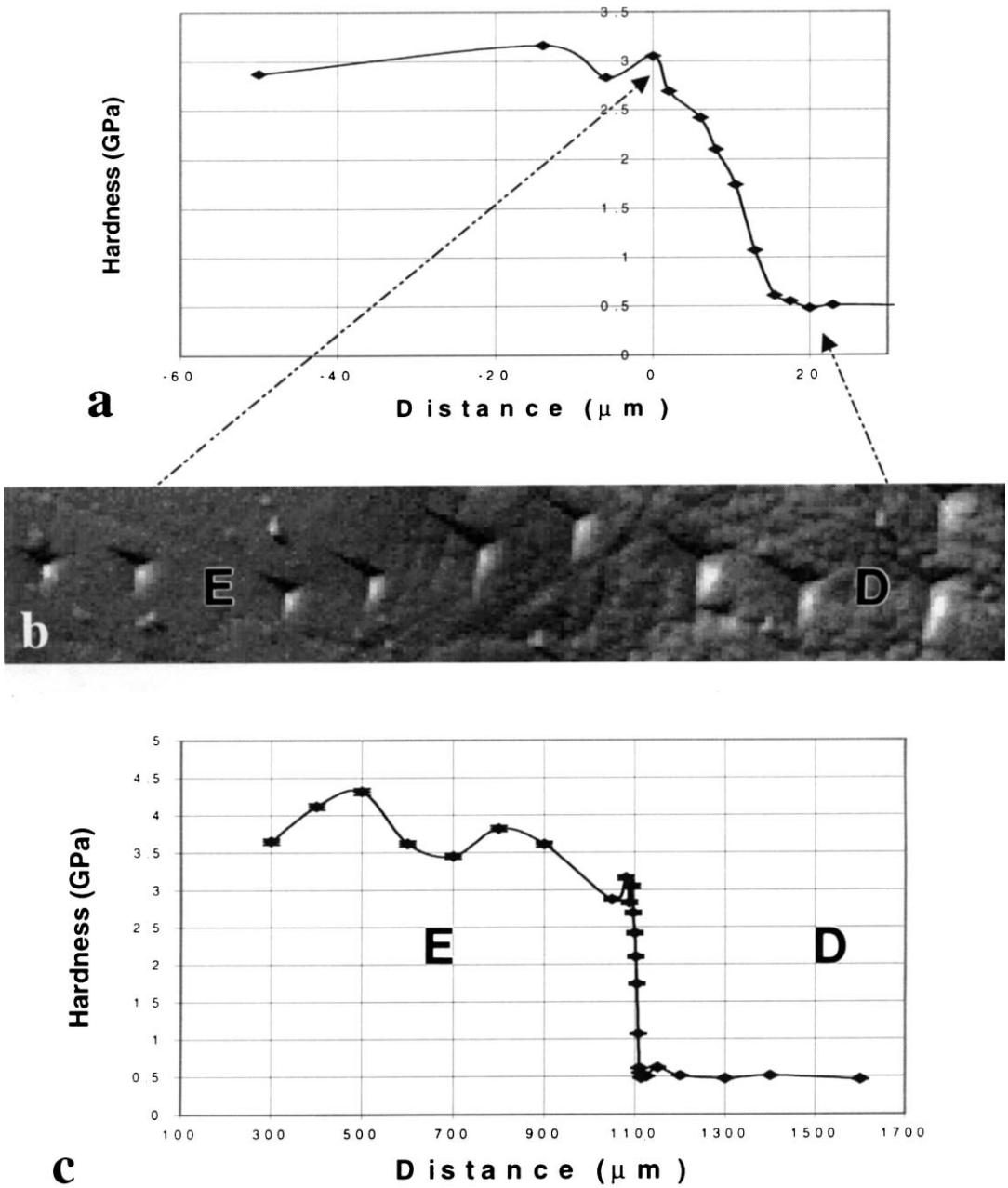

Fig. 5. (a) An example of an indentation profile across DEJ and (b) the corresponding indentations (AFM image, height variations). (c) The same profile, showing the full extend of the profile from enamel (E) to dentin (D).

crostructural inhomogeneities (such as closeness to the DEJ), and (iii) appropriateness of the indentation sizes for sampling relevant regions. Roughness is a major factor that can influence the values obtained by nano-indentation tests. This is because the disparities on the sample surface could convolute with the shape of the indenter tip which would result in lower hardness (or moduli) values. In a scanned area of 50×50 μm, the rms value of the surface roughness imaged by the Berkovich tip was in the order of 70 nm after polishing with 0.25-μm diamond paste. However for an area of (2×2 μm), rms roughness was mostly $\sim$ 5 nm or less. The rms roughness data determined by the diamond tip of the nano-indenter was considered sufficiently accurate because its tip radius was 50 nm, comparable to the mean particle diameter of the grinding media. Indentations were made on positions where local rms roughness of enamel was about 5 nm or less and that of dentin was about 15 nm. As can be seen from the indentations in Fig. 3, the depth scale of the surface features induced by polishing (e.g., surface scratches) is small compared to the size of the indentations. For the indentation depth of 100 nm, the standard deviations in H and E were $\pm$5% or less in both enamel and dentin. The high accuracy in the measurements indicates the success of

polishing of the samples that resulted in highly smooth surfaces and only the limited effects of the surface roughness on the tests results.

It should be pointed out that 0.05 μm alumina powder was also used to further reduce surface roughness. However this attempt was unsuccessful because the colloid alumina suspension had to be kept at a pH of 3.0 in order to avoid agglomeration of alumina (corundum) particles. Because of the acidic nature of such a suspension, dentin was preferentially etched during the polishing process; as a result, a step was created between dentin and slightly etched-enamel regions.

Proper spacing between indents is also important to ensure that the measurements are not influenced by the overlap of the adjacent indentations. Successive indents too close to each other can affect the measurements in two ways. An indentation to be made that is too close to an existing indent can result in either softening due to tip overlap over the preexisting cracks induced during the previous indentations, or hardening due to the work-hardened proximity regions around the preexisting indent. In our experiments, microcracks were not observed even upon indentations made using the largest loads (2500 μN) and largest indentation widths (up to 1 μm size) (Fig. 3). In work-hardenable materials it is known that the region around the periphery of an indent, up to several times the diameter of the indentation, is strain-hardened, for example, due to dislocation tangles (e.g., in metals) or amorphous to solid transformation (e.g., in polymers) [19]. Thus, adjacent indents should be apart from each other at least 3–5 times the indentation diameter. Ceramic materials such as HAP and organic fibrous polymers such as collagen are not known to work-harden. However, an amorphous material and a polymer matrix could be crystallized locally and porous polycrystalline ceramics can be significantly densified locally under an applied load. Consequently, either enamel or HAP/collagen composite materials in tooth may deform by some unknown mechanism(s) in the vicinity of the indentor, thereby modifying the local structure of the sample. Therefore, precautions have to be taken to avoid close proximity of successive indentations. In our experiments, where the indentation diameter was ~0.8 μm, the closest center-to-center spacing between indents was 2 μm, i.e., about three times the diameter of an indentation. This average separation between the successive indents in local regions of each of the two tissues was adequate to eliminate any possible local deformation effect.

The choice of the size of indentations is also relevant since it determines whether the indentation data are meaningful in reflecting the local microstructural property. If the indentation size is too small (smaller than the hard, filling, component of the composite) than the nano-mechanical properties will reflect only those of the filler material and not the overall composite [19,20]. The HAP crystals (i.e., the filler phase) are ~50 nm thick in enamel and ~3 nm thick in dentin. Therefore, an indentation size of 100 nm deep by 0.8 μm in diameter used in our experiments were considered to be large enough to characterize the DEJ zone as well as both the dentin and the enamel regions on either side of the DEJ zone.

The downward trend in the mechanical properties profiles determined in this work (Figs. 4 and 5) is consistent with the sonic velocity profiles across DEJ zone obtained from bovine teeth [3] as bovine dentin and enamel appear to be just as anisotropic as are human tissues. The profiles obtained from human teeth in this work suggests that there are continuous changes in microstructure in the DEJ region as opposed to an abrupt change between the enamel and dentin phases. There are variable amounts of dentin and enamel admixture; their relative ratios change continuously in the area adjacent to the DEJ. In addition, an imaginary interface taken between the dentin and enamel regions parallel to the DEJ zone is not a straight line, but rather, it zigzags along the DEJ zone. Furthermore, this imaginary line may also meander in the subsurface region (i.e., above and below the projection seen in the AFM images). The interpenetration of dentin and enamel tissues with one another can be seen in the AFM images (Figs. 2 and 5). Fig. 2 displays islands of enamel (flat domains with parallel lines, indicated by arrows) scattered within dentin indicating a possible three-dimensional interpenetrating network of dentin and enamel. The extent of interpenetration of the two tissues cannot be quantitatively determined from the AFM image alone since these images only display two-dimensional features through the interface sections representing a single projection of the structure. A technique that can provide three-dimensional imaging is needed for full evaluation of the extend of interpenetration between dentin and enamel, and correlate it to the physical properties of the DEJ zone. Imaging techniques that are predicted to be helpful are X-ray microtomography or high voltage transmission electron microscopy (HVEM). In X-ray microtomography, a submicron probe is needed which may be obtained using a synchrotron source. In HVEM, thick successive (ultramicrotomed) sections would be useful for analysis to obtain a pseudo-three-dimensional structural data. Nevertheless, from the indentation profiles obtained in this work (Figs. 4 and 5), estimated overlapping zone is in the range of 15–25 μm. As indicated previously, indentation profile corresponding to the transition region at the DEJ cannot be represented by a single, smooth, universal function. It may be more realistic to consider the DEJ zone to have a variable structure (and width) depending on its location on the *ZX* section of the interface along either of the orthogonal directions ($\bar{x}$ and $\bar{z}$ in Fig. 1b) at a given dentin–enamel interface region.

A mammalian tooth exhibits functionally-graded properties because of its hard, exterior enamel, and tough, interior dentin. Micromechanically, therefore, the tooth is expected to have a strong mechanical bond at the interface between enamel and dentin. The mechanical coupling, as

evidenced by the S-shaped profile of nano-mechanical properties found in this work, is predicted to reflect the ability of the structure to prevent fracture or delamination at the interface region where stress concentration would build when subjected to chewing. Hard enamel, in addition to being wear resistant, would transfer the load through its rigid structure towards the interior, finally being transferred through the DEJ zone into the tough dentin where the stresses would be relieved by the relatively soft structure. An overlapping structure (as observed), with an interpenetrating architecture rather than a flat one at the DEJ, could be an essential feature for the transfer of load from enamel to dentin and its eventual dissipation in dentin. The micro-architectural design of the DEJ probably leads a strong (but flexible and, therefore, tough) mechanical bond between enamel and dentin and, hence, provide an efficient coupling between these mechanically and structurally different composites.

In dentin, the filler HAP nano-crystallites are short, relatively flat and randomly organized in the composite structure. In enamel, relatively larger HAP crystallites are long and form rod-like structures that are crystallographically and morphologically textured producing a different type of composite material. Although enamel and dentin tissues interpenetrate into each other at the DEJ, the extend of the structural coupling between the inorganic fillers is not yet fully understood. In addition, there is a lack of knowledge of structural correlation (if any) of the organic matter in the two tissues between the organic components that constitute the matrices. Therefore, detailed analysis, by various microscopy techniques and spatial resolution levels, provided by TEM (nm), AFM (sub-μm), and X-ray microtomography (μm), is desirable to fully characterize hierarchical structures of the DEJ from the nanometer- to the macro-scales and to establish the true nature of mechanical bridging between the highly organized enamel and dentin structures of human teeth.

5. Conclusion

Nano-hardness and elastic moduli profiles were established in sub-micron spatial dimensions across DEJ junction on sectioned human incisor teeth samples. The nano-mechanical property profiles were obtained by using a nano-indenter apparatus attached to an AFM. This nano-mechanical testing system provided high precision in terms of accurate positioning of the indenter on local regions of the sectioned samples, application of the appropriate μN-level loads on dentin and enamel regions, and obtaining load–depth curves from many points across the dentin–enamel junction zone. The S-shaped hardness profiles start out at fairly high values ($\sim$ 4.80 GPa) and are relatively uniform in enamel; they gradually decrease across the DEJ and reduced to a value of $\sim$ 0.80 GPa in dentin. The elastic modulus profiles, from corresponding regions, also follow a similar specific trend. Based on these measurements and AFM imaging of sectioned and polished samples, we estimate the width of DEJ to be in the range of 15–25 μm. The DEJ region is a zone of interpenetrating tissues, containing both enamel and dentin domains. Micromechanically, enamel is hard and dentin is soft. Therefore, the interpenetrating structure at the interface is expected to promote continuous load transfer across the DEJ zone and provide the mechanical coupling that is essential in reducing multiaxial interfacial stresses that will otherwise form cracks between these two biological hard tissues. Detailed electron microscopy, AFM, and X-ray tomography studies of the DEJ are required to fully understand the three-dimensional structural integration of the two tissues across this interface. Once established, a detailed structure–property correlation across the DEJ would then provide a strong basis for the design of better artificial enamel implants and, potentially, for biomimetic tissue regeneration via controlled biomineralization.

Acknowledgements

We acknowledge the financial support through AASERT Program through ARO grant # DAAH04-95-1-0279 and NIDCR grant #DE60390 through NIH.

References

[1] P.W. Lucas, in: B. Kurten (Ed.), Basic Principles of Tooth Design, Teeth, Form, Function, Evolution, Columbia Univ. Press, New York, 1979, pp. 154–162.
[2] N.E. Waters, Some mechanical and physical properties of teeth, in: J.F.V. Vincent, J.D. Currey (Eds.), Mechanical Properties of Biological Materials, Cambridge Univ. Press, Cambridge, UK, 1980, pp. 99–135.
[3] R.Z. Wang, S. Weiner, Strain-structure relations in human teeth using Moire fringes, J. Biomech. 31 (2) (1998) 135.
[4] H.C. Hodge, H. McKay, The microhardness of teeth, JADA 227 (1933).
[5] R.G. Craig, F.A. Peyton, The microhardness of enamel and dentin, J. Dent. Res. 37 (4) (1958) 661.
[6] S.T. Rasmussen, R.E. Patchin, Fracture properties of human enamel and dentin in an aqueous environment, J. Dent. Res. 63 (12) (1984) 1362.
[7] P.G. Fox, The toughness of enamel, a natural fibrous composite, J. Mater. Sci. 15 (1985) 3113.
[8] O.M. El Mowafy, D.C. Watts, Fracture toughness of human dentin, J. Dent. Res. 65 (5) (1986) 677.
[9] C.P. Lin, W.H. Douglas, Structure–property relations and crack resistance at a bovine dentin–enamel junction, J. Dent. Res. 73 (5) (1994) 1072.
[10] N. Meredith, M. Sheriff, D.J. Setchell, S.A.V. Sivanson, Measurements of the microhardness and Young modulus of human enamel and dentin using an indentation technique, Arch. Oral Biol. 41 (6) (1996) 539.
[11] J.H. Kinney, M. Balloch, S.J. Marshall, G.W. Marshall, T.P. Wehs, Atomic force microscope measurements of the hardness and elasticity of peritubular and intertubular human dentin, J. Biomech. Eng. 118 (1996) 133.

[12] H.H.K. Xu, D.T. Smith, S. Jahanmir, E. Romberg, J.R. Kelly, V.P. Thompson, E.D. Rekow, Indentation damage and mechanical properties of human enamel and dentin, J. Dent. Res. 77 (3) (1998) 472.
[13] R.Z. Wang, S. Weiner, Strain-structure relations in human teeth using Moire fringes, J. Biomech. 31 (2) (1998) 135.
[14] C.P. Lin, W.H. Douglas, S.L. Erlandsen, Scanning electron microscopy of Type-I collagen at the dentin–enamel junction of human Teeth, J. Histochem. Cytochem. 41 (3) (1993) 381.
[15] H. Fong, M. Sarikaya, Nanoscale Correlation of Structure and Mechanical properties of a Human Tooth, Microscopy and Microanalysis, '98, Springer, New York, 1998, p. 942.
[16] W.C. Oliver, G.M. Pharr, An improved technique for determining hardness and elastic modulus using load and displacement sensing indentation experiments, J. Mater. Res. 4 (6) (1992) 1564.
[17] M.F. Doerner, W.D. Nix, A method of interpreting the data from depth-sensing indentation instruments, J. Mater. Res. 1 (4) (1986) 601.
[18] S.N. White, M.L. Paine, W. Luo, M. Sarikaya, H. Fong, Z. Yu, Z.C. Li, M.L. Snead, The dentino-enamel junction is a broad transitional zone uniting dissimilar bioceramic composites, J. Am. Ceram. Soc. 83 (2000) In Press.
[19] D. Hull, An Introduction to Composite Materials, Cambridge Univ. Press, Cambridge, UK, 1981.
[20] S. Komarneni, J.C. Parker, G.J. Thomas (Eds.), Nanophase and Nanocomposite Materials, Proc. of MRS, Vol. 286, Materials Research Society, Pittsburgh, PA, 1993.